

# Structure and Mechanical Property of Friction-Stir Weld Joint of 2195-T8 Al-Li Alloy Plate

Li Jinfeng<sup>1</sup>, Chen Yonglai<sup>2</sup>, Zhang Xuhu<sup>2</sup>, Zheng Ziqiao<sup>1</sup>

<sup>1</sup> Central South University, Changsha 410083, China; <sup>2</sup> Aerospace Research Institute of Materials and Processing Technology, Beijing 100076, China

**Abstract:** The tensile properties of friction stir weld (FSW) joint of 2195-T8 Al-Li alloy plate with 5 mm thickness prepared by straight-cylindrical (SC) pin and threaded-cylindrical (TC) pin at different rotational speeds and welding speeds were investigated. The structures of the FSW joint were detected. Results show that when prepared by SC pin at improper welding speed, continuous hole is formed in the FSW joint along the welding direction, leading to lower joint strength. TC pin alleviates the formation of hole in the weld, and the joint strength is enhanced with the rotational speed increasing from 700 to 1100 r/min at a given welding speed of 120 mm/min. The grains in the nugget zone (NZ) are recrystallized, but their size is inhomogeneous. The precipitates of T1 (Al<sub>2</sub>CuLi) and  $\theta'$  (Al<sub>2</sub>Cu) in the NZ are completely dissolved. All  $\theta'$  precipitates but most T1 precipitates are dissolved in the thermo-mechanically affected zone (TMAZ). Meanwhile, dislocations are formed in the NZ.

**Key words:** 2195 Al-Li alloy; friction stir weld (FSW); mechanical property; structure

Friction stir welding (FSW), a solid state joining process with energy efficiency, versatility and being environment friendly, was developed and patented by The Welding Institute (TWI) in 1991<sup>[1,2]</sup>. In comparison with other welding techniques, FSW offers advantages for low residual stresses, low distortion, defect-free and high joint strength<sup>[3,4]</sup>. A lot of work show great influence of FSW parameters such as rotational speed, welding speed and axial force on the structure and strength of the FSW joint<sup>[5-7]</sup>. Meanwhile, tool pin profiles affect the plastic flow of metal during the FSW process and therefore influence the joint properties<sup>[8-10]</sup>.

Al-Li alloys with low density, high specific strength and modulus, low fatigue-crack growth rate were applicable to aircraft and aerospace structures<sup>[11]</sup>. Recently, the application of Al-Li alloys around the world will be inevitably expanded in aircraft and aerospace structures. Because of the high activity and evaporation of Li during fusion welding, the FSW will be the most potential welding technique for Al-Li alloys.

Al-Cu-Li alloys containing micro-alloying elements of Mg and Ag are one of the most important series of Al-Li alloys which include 2195, 2050 and 2198. All these alloys have been used or will be used in aerospace tank. In this case, the influence of rotational speed and welding speed on the structure and strength of the 2195 Al-Li alloy FSW joint was investigated.

## 1 Experiment

The as-received 2195-T8 Al-Li alloy plates with 5 mm thickness were cut into the required size (250 mm×100 mm). Square butt joint configuration (Fig.1a) was prepared to fabricate FSW joints by a numerical control gantry type friction stir welding machine developed by Central South University. Single pass welding procedure was operated and the welding direction was vertical to the rolling direction. Straight-cylindrical (SC) pin and threaded-cylindrical (TC) pin (Fig.1b) with a pin diameter of 5 mm and a shoulder diameter of 12 mm were used to fabricate the joints. For different tool pins, the FSW parameters are shown in Table 1.

Received date: March 30, 2017

Foundation item: Teacher's Research Foundation of Central South University (2013JSJJ001); National High Technology Research and Development Program of China (2013AA032401)

Corresponding author: Chen Yonglai, Ph. D., Professor, Aerospace Research Institute of Materials and Processing Technology, Beijing 100076, P. R. China, E-mail: [chenyonglai@263.net](mailto:chenyonglai@263.net)

Copyright © 2018, Northwest Institute for Nonferrous Metal Research. Published by Elsevier BV. All rights reserved.

Meanwhile, the axial force was fixed as 12 kN.

After 15 d at room temperature, the tensile samples were cut from the FSW joint (Fig.1). The typical parallel gauge dimensions for tensile measurement were 30 mm in length and 8 mm in width. The tensile tests were carried out by an MTS 858 testing machine at a tensile speed of 2 mm/min. It should be noted that measuring the elongation is difficult, because the plastic deformation only occurs at the weld during the tensile process. So, the elongation was measured according to the following two manners. (1) The shoulder diameter was selected as the original length, which was much close to the weld width, and the corresponding elongation was defined as EL-1. (2) The length of parallel segment was selected as the original length, and the corresponding elongation was defined as EL-2, which can be used for evaluation.

The fracture surface was observed by a scanning electron microscope (SEM). The transverse section was ground and polished, and then the micro-morphologies were observed using a Leica metallographic microscope. The microstructures were observed with a Tecnai G<sup>2</sup>20 Transmission Electron Microscope (TEM).

Electron Backscatter Diffraction (EBSD) was used to analyze the grain size in the joint. The EBSD data acquisition was performed using a Sirion 200 Field Emission Gun Scanning Electron Microscope (FESEM) equipped with XM4-Hikari electronic backscatter signal collection system. The OIM Analysis 5.3 software was used to analyze the received EBSD data.

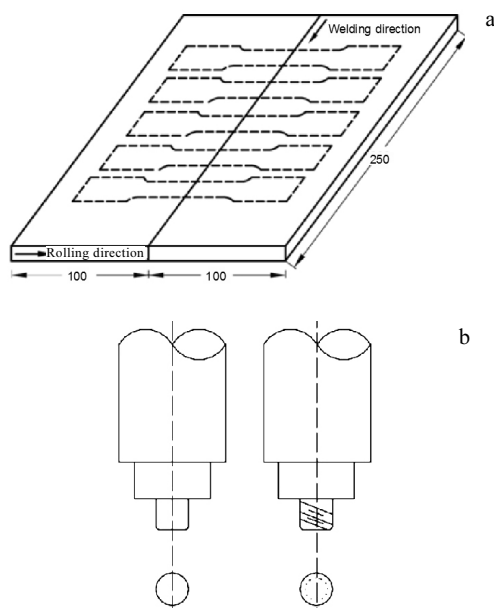


Fig.1 Square butt joint configuration and tensile samples (a) and tool pin profiles (SC and TC) (b)

Table 1 Welding parameters for FSW of 2195-T8 Al-Li alloy

Tool pin	Welding speed/mm·min <sup>-1</sup>	Rotational speed/r·min <sup>-1</sup>
SC	60, 90, 120, 150, 180	1000
TC	120	700, 800, 900, 1000, 1100

## 2 Results and Discussion

### 2.1 Effect of welding speed on the FSW strength

Table 2 shows the tensile properties of the FSW joint prepared by the SC pin at different welding speeds with a given rotational speed of 1000 r/min. The yield strength is enhanced with the welding speed. The tensile strength is enhanced with the welding speed increasing from 60 to 120 mm/min. However, with further increase of the welding speed, the tensile strength is lowered. Meanwhile, it is found that all of the tensile specimen the tensile fracture always occurs in the advancing side (Fig.2).

The joint strength variation is associated with the defect at different welding speeds. Fig.3 shows the sectional images of the FSW joint prepared at different welding speeds. At the welding speed of 60 mm/min, there exists a hole at the bottom of the advancing side (white circle) (Fig.3a). As the welding speed is increased to 90 and 120 mm/min, this defect is gradually decreased (Fig.3b). However, as the welding speed is further increased to 150 and 180 mm/min, this defect is aggravated again (Fig.3c).

Fig.4 shows the SEM fracture morphologies of the FSW joint prepared by the SC pin at different welding speeds. There exists a continuous tunnel (white dash line) on the fracture surface of the joint prepared at 60 mm/min welding speed (Fig.4a), indicating that the hole defect in Fig.3a is a continuous hole. As the welding speed is increased to 120 mm/min, this continuous tunnel is not found (Fig.4b). However, at the welding speed of 150 and 180 mm/min, it appears again (figure omitted).

The tensile properties (Table 2) and joint defect (Fig.3) dependence on the welding speed can be explained by the following two factors. The first factor is associated with the metal flow. During the FSW process, the tool rotation opposes the traversing weld direction in the retreating side of the weld. Due to the frictional forces between the tool shoulder and the substrate, the surface material is displaced in both the rotational direction and the welding direction.

In the retreating side, the surface material rotating with the tool shoulder is therefore forced to flow under material moving in the welding direction<sup>[12]</sup>. In essence, the FSW tool shoulder extrudes a volume of surface material from the retreating side into the plasticized region of the joint around the pin and under the tool shoulder. The FSW nugget development has been developed as an extrusion process<sup>[13,14]</sup>.

**Table 2** Tensile properties of the joint prepared by SC pin at a given rotational speed of 1000 r/min with different welding speeds

Welding speed/ mm·min <sup>-1</sup>	Yield strength/ MPa	Tensile strength/ MPa	Elongation/%	
			EL-1	EL-2
60	246	353	8.7	3.5
90	258	338	10.4	4.2
120	268	379	13.4	5.7
150	269	343	11.1	4.5
180	271	332	10.4 <td 4.2	

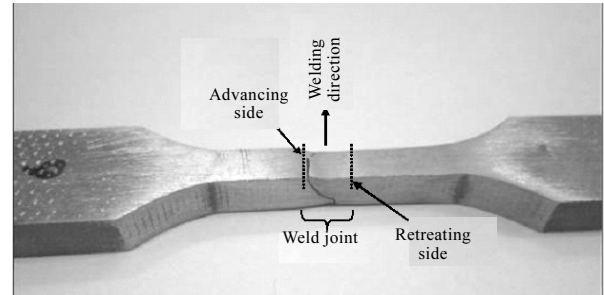


Fig.2 Fracture location of the FSW joint of 2195 Al-Li alloy

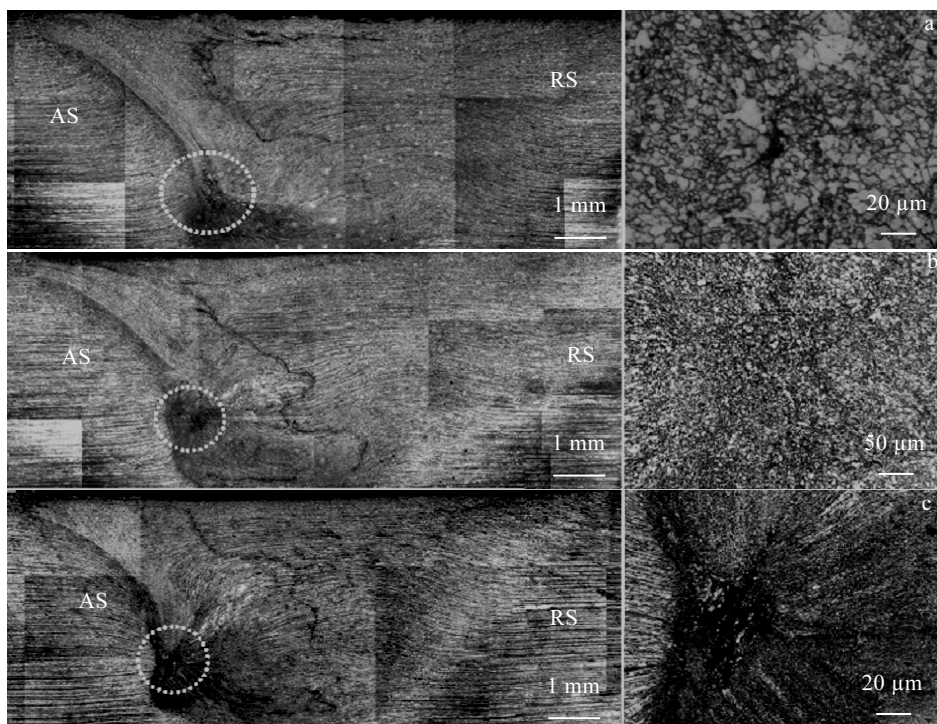


Fig.3 Sectional images of the joint prepared by SC pin at a given rotational speed of 1000 r/min with welding speeds of 60 mm/min (a), 120 mm/min (b), and 150 mm/min (c) (left part shows the whole joint, and right part is the enlargement the white circle)

The nugget forms as a volume of material from the weld surface which is extruded into the joint during each revolution of the tool. As the tool continues to rotate and traverse, more material is extruded into the region, forcing the buckled, extruded columns further into the plasticized zone and introducing new material into the region. At a slower welding speed, the pressure at the pin front is small, resulting in a smaller friction force. The amount of surface material extruded to the retreating side and then to the plasticized region from the retreating side is smaller. This factor causes the defect at the bottom of the advancing side and a lower strength of the joint. As the welding speed is increased, the pressure at the pin front is increased and

therefore the extrusion is increased, the plastic flow from the retreating side to the advancing side is improved and the strength is enhanced to a certain degree. The strength of the FSW joint at welding speed of 120 mm/min is therefore higher.

However, as the welding speed is further increased to higher than 150 mm/min, the other factor plays a greater role. Higher welding speeds are associated with low heat inputs within per unit length, resulting in faster cooling rate. That is to say, the softened area in FSW is narrower at the higher welding speed than that at the lower welding speed. At high welding speeds of 150 mm/min and 180 mm/min, low heat input therefore causes lack of bonding

and the formation of hole defects in the advancing side and yields poor strength.

## 2.2 Effect of rotational speed on the FSW strength

Table 3 shows the tensile properties of the joint prepared by the TC pin at different rotational speeds with a given welding speed of 120 mm/min. As the rotational speed is increased from 700 to 1100 r/min, the tensile strength is increased from 267 to 430 MPa, and the elongation is also greatly increased.

Fig.5 shows the sectional picture of the joint prepared at different rotational speeds. At the rotational speed of 700~900 r/min, there are still some small holes at the bottom of the advancing side (Fig.5a). However, the hole disappears at the rotational speed of 1100 and 1200 r/min (Fig.5b).

Compared to the joint prepared by the SC pin, the hole defect in this joint is isolated. This is associated with the heat and plastic flow improvement caused by the TC pin. There exists screw thread on the pin surface, which generates more heat than the SC pin. Meanwhile, the screw thread exerts an extra downward movement to the plasticized metal [15]. In addition, it also causes screw flow of plastic metal along the screw, i.e. plastic flow from the retreating side to the advancing side. These factors promote the plastic flow and therefore alleviate the defect in the joint.

As prepared by the TC pin, the joint strength is greatly influenced by the rotational speed. This is mainly associated with the different heat input. In FSW, spin rotation results in stirring and mixing of material around the rotating pin which in turn elevates the metal temperature. The maximum temperature is a strong function of the rotational speed. When the rotation speed increases, the heat input within the stirred zone increases due to the higher friction heat which in turn results in more intense stirring and mixing of materials [13], and therefore enhances the joint strength.

It is of interest that the enhancement in yield strength is different from that in tensile strength. As the rotational speed is increased from 700 to 1100 r/min, the enhancement of the tensile strength is significantly higher than that of the yield strength. The tensile strength is enhanced by 163 MPa, but the yield strength is only enhanced by 38 MPa. To evaluate the joint strength, the strength of solutionized and T3 treated 2195 Al-Li alloy is listed in Table 3. Both the tensile strength and the yield strength of the joint prepared by the appropriate parameters (1100 r/min rotation speed and 120 mm/min welding speed) are increased by 16% compared to those of the 2195-T3. This strength enhancement feature is related to the microstructures and bonding, which will be discussed in the following section.

## 2.3 Structures of the FSW joint

Fig.6 shows the metallographic pictures of the FSW joint

prepared by the TC pin at a welding speed of 120 mm/min with a rotational speed of 1100 r/min. As same as the substrate (Fig.6a), the grains in the HAZ (heat-affected zone) retain elongated shape (Fig.6b). While, in the TMAZ, the grains are deflected from the bottom to the top (Fig.6c).

The grains in the NZ are recrystallized, forming fine and equi-axed grains. However, the recrystallized grain size is inhomogeneous. The grain at the top (Fig.7a) is a little larger than that in the bottom (Fig.7b). This phenomenon was also observed in the FSW joint of other Al alloys [14,16].

Fig.8 shows the metallographic images of the NZ from

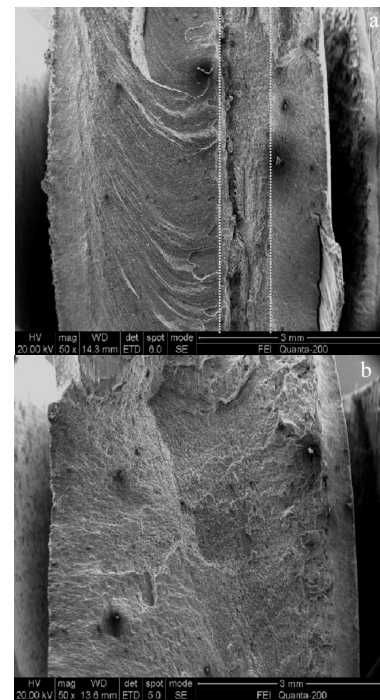


Fig.4 SEM fracture morphologies of the FSW joint prepared by SC pin at a given rotational speed of 1000 r/min with welding speeds of 60 mm/min (a) and 120 mm/min (b)

**Table 3 Tensile properties of the joint prepared by TC pin at a given welding speed of 120 mm/min with different rotational speeds**

Rotational speed/r·min <sup>-1</sup>	Yield strength/MPa	Tensile Strength/MPa	Elongation/%	
			EL-1	EL-2
700	259	267	8.4	3.4
800	274	292	9.1	3.6
900	284	339	10.9	4.4
1100	297	430	19.5	8.3
1200	290	421	14.9	6.0
Solutionized	182	351	25	
2195-T3	250	360	14	
2195-T8	538	565	6	

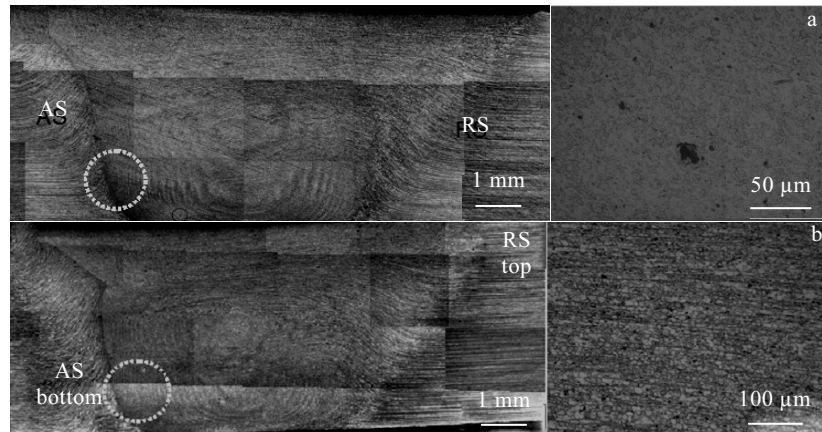


Fig.5 Sectional pictures of the joint prepared at a given welding speed of 120 mm/min with rotational speeds of 800 r/min (a) and 1100 r/min (b) (Left part shows the whole joint, and right part is the enlargement of the white circle)

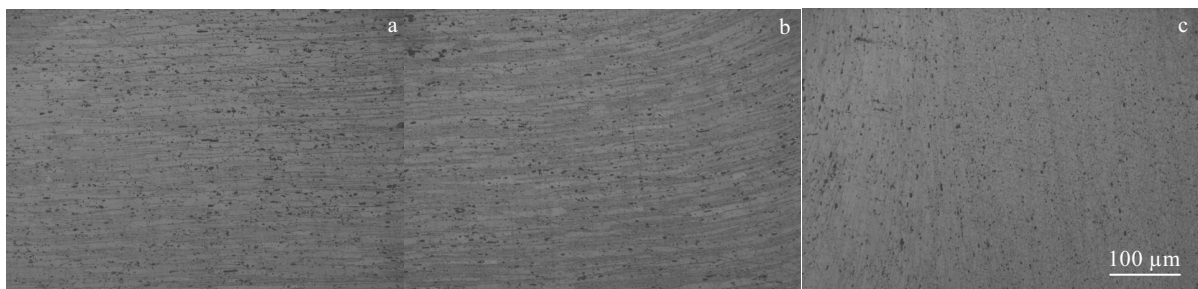


Fig.6 Metallographic images of the FSW joint of 2195-T8 Al-Li alloy: (a) substrate, (b) location containing HAZ and TMAZ in the advancing side, and (c) location containing TMAZ and NZ

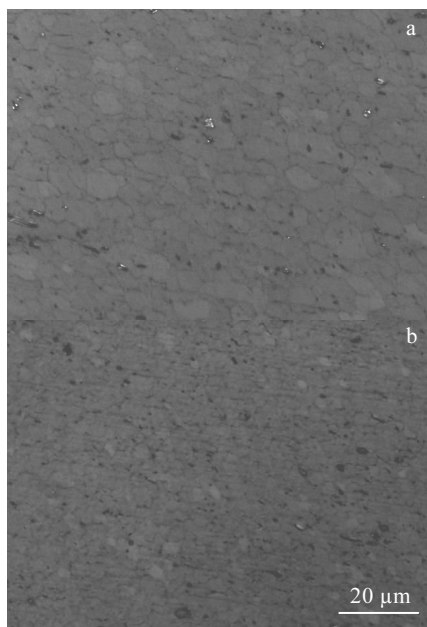


Fig.7 Metallographic images of top NZ (a) and bottom NZ (b)

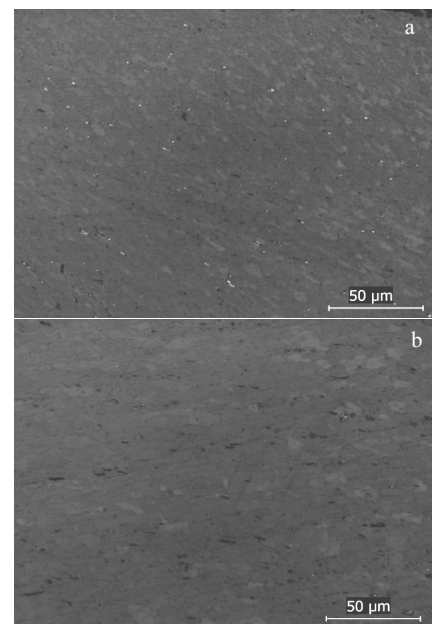


Fig.8 Metallographic images of NZ adjacent to TMAZ in the advancing side (a) and central NZ (b)

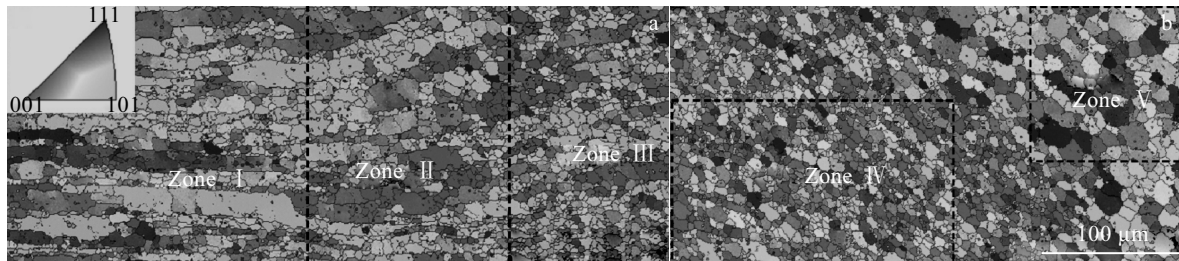


Fig.9 EBSD images of the joint at different locations: (a) location containing HAZ and TMAZ in the advancing side; (b) NZ

**Table 4** Area fraction of grains with different size range at various FSW joint locations (%)

Zone	$\leq 10 \mu\text{m}$	10~20 $\mu\text{m}$	20~30 $\mu\text{m}$	$\geq 30 \mu\text{m}$
I	37.2	30.5	11.8	20.5
II	44.8	36.7	18.5	-
III	79.6	20.4	-	-
IV	93.5	6.5	-	-
V	57.5	42.5	-	-

the advancing side to the retreating side, which also indicates the non-uniformity of the recrystallized grain size. The grain size of the NZ adjacent to the TMAZ in the advancing side (Fig.8a) is smaller than that of the central NZ (Fig.8b). Then, it is decreased a little in the retreating side (figure omitted). This grain size variation should be mainly associated with the temperature distribution at different locations.

The recrystallized grain size distribution is reflected more distinctly by EBSD observation, as shown in Fig.9. The grains in the HAZ (Zone I) keeps elongated shape, and those in the TMAZ in the advancing side (Zone II and Zone III) are deflected. The grains in the TMAZ are partly dynamically recrystallized, and from Zone II to Zone III, the recrystallization fraction is increased. In the NZ, all the grains are recrystallized, but the grains in the central NZ (Zone V) is obviously larger than those in the NZ adjacent to the TMAZ (Zone IV), as shown in Table 4.

Fig.10 shows the TEM images of the substrate and HAZ.

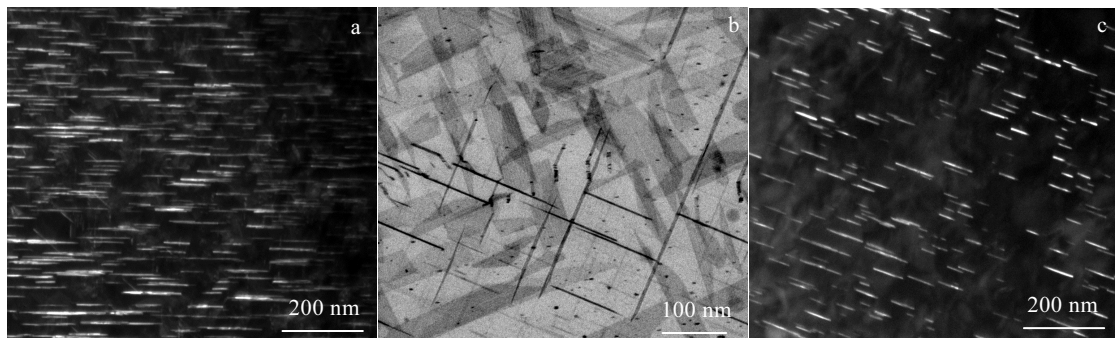


Fig.10 TEM images of the 2195-T8 Al-Li alloy substrate and HAZ: (a) dark field image of T1 precipitates in the substrate; (b) bright field image of  $\theta'$  precipitates in the substrate; (c) dark field image of T1 precipitates in HAZ

In the substrate, the main strengthening precipitates are T1 ( $\text{Al}_2\text{CuLi}$ ) (Fig.10a) and  $\theta'$  ( $\text{Al}_2\text{Cu}$ ) (Fig.10b). In addition, the alloy is micro-alloyed by Zr element, and  $\beta'$  ( $\text{Al}_3\text{Zr}$ ) precipitates absolutely exist<sup>[17]</sup>. In the HAZ, T1 precipitates still account for a high fraction (Fig.10c). However, due to the high temperature caused by friction and stirring of the tool pin, T1 precipitates are partly redissolved, and their fraction is decreased. Meanwhile, maybe because of their small amounts, it is difficult to observe  $\theta'$  precipitates in the HAZ.

Inside the TMAZ, most precipitates are re-dissolved. Fig.11 shows the bright field TEM images of the TMAZ adjacent to the NZ. Only a very small number of T1 precipitates are observed (Fig.11a), and  $\theta'$  precipitates are completely dissolved. Meanwhile, plastic deformation occurs, there exist sub-grains and some dislocations are found in the sub-grains (Fig.11b).

In the NZ, both T1 and  $\theta'$  precipitates are completely re-dissolved. However, some rod-shaped particles are observed (arrows in Fig.12a), which are identified as  $T_B$  ( $\text{Al}_7\text{Cu}_4\text{Li}$ ) precipitates<sup>[17]</sup>. Meanwhile, a great number of helical dislocations are observed (Fig.12b).

The above structure variation at the joint influences the hardness distribution. The hardness distribution of the joint displays a W-shaped characteristic at the transverse section (Fig.13). The hardness is decreased greatly from the substrate to the HAZ and TMAZ. Then, it is increased a

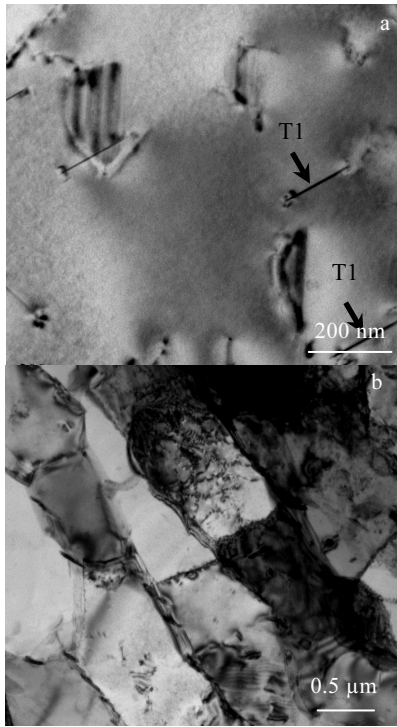


Fig.11 TEM bright field images of TMAZ adjacent to NZ: (a) bright field image of grain interior T1 precipitates and (b) sub-grains

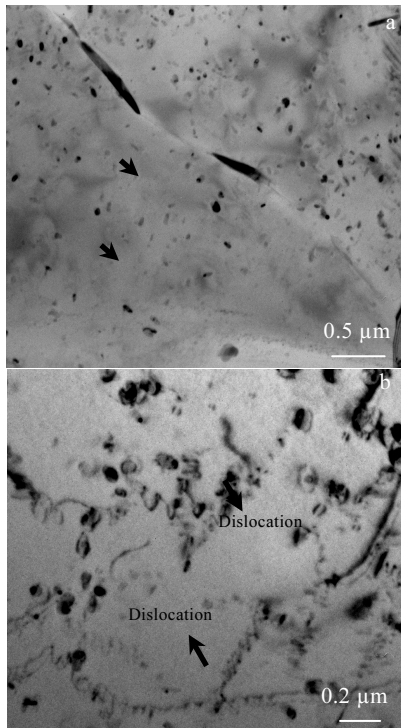


Fig.12 TEM bright field images of NZ: (a) particles and (b) helical dislocations

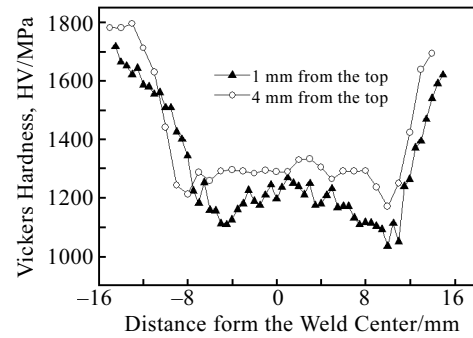


Fig.13 Hardness distribution of the FSW joint at the cross section

little at the NZ. This hardness distribution is dependent on the precipitate difference. From the substrate to the HAZ and TMAZ, the re-dissolution of the strengthening precipitates is increased gradually (Fig.10~Fig.11), which leads to a decrease in the hardness from the substrate to the TMAZ. Meanwhile, a small hardness increase in the NZ is consistent with its higher dislocation density (Fig.12b). Along the thickness direction, the hardness at the top is a little lower than that at the bottom, which should mainly be caused by the grain structure difference (Fig.7).

The tensile properties of the joint are determined by the above structures. On the one hand, due to lack of strengthening precipitates of T1 and  $\theta'$ , the strength, especially the yield strength of the NZ is much lower than that of the substrate. The plastic deformation during tensile process therefore mainly occurs on the NZ. On the other hand, the microstructure of the NZ is a little similar to that of 2195-T3, i.e. the strengthening precipitates of T1 and  $\theta'$  are not found in both the 2195-T3 and the NZ. The main difference lies in that the NZ possesses fine equiaxed grains, but the grains in 2195-T3 are elongated. Meanwhile, the dislocation density in the NZ should be higher than that in 2195-T3. These two factors result in that the joint strength is higher than that of 2195-T3 to a certain extent. However, its yield strength can not be enhanced substantially due to lack of the strengthening precipitates T1 and  $\theta'$ . In addition, the fracture of the tensile sample is also dependent on the bonding. Proper FSW parameters eliminate (D4 and D5 in Table 3) eliminate the lack of bonding and the hole defects, and then greatly enhance the tensile strength (Table 3).

### 3 Conclusions

1) As prepared by SC pin at lower welding speed (60~90 mm/min) and higher welding speed (150~180 mm/min), continuous hole is formed in the FSW joint along the welding direction, leading to its lower tensile strength.

2) TC pin alleviates the hole defect in the weld joint. The FSW tensile strength is enhanced with increasing the rotational speed from 700 to 1100 r/min at a given welding speed of 120 mm/min.

3) The grains in the NZ are recrystallized, but their size distribution in NZ is non-uniform. It is decreased along the direction from the top to the bottom. Meanwhile, the grain size in the NZ adjacent to the TMAZ is smaller than that in the central NZ.

4) The precipitates of T1 and  $\theta'$ , the main strengthening precipitates in 2195-T8 Al-Li alloy substrate, are completely dissolved in the NZ. In the TMAZ, most T1 precipitates but almost all  $\theta'$  precipitates are dissolved. Meanwhile, helical dislocations are formed in the NZ.

## References

- 1 Thomas W M, Nicholas E D, Needham J C et al. *GB Patent*, 9125978.8 [P]. 1991
- 2 Xu Xiangyang. *Rare Metal Materials and Engineering*[J], 2009, 38(S1): 213 (in Chinese)
- 3 Bitondo C, Prisco U, Squilace A et al. *International Journal of Advanced Manufacturing Technology*[J], 2011, 53(5-8): 505
- 4 Cai B, Zheng Z Q, He D Q et al. *Journal of Alloys and Compounds*[J], 2015, 649: 19
- 5 Radisavljevic I, Zivkovic A, Radovic N et al. *Trans Nonferrous Met Soc China*[J], 2013, 23(12): 3525
- 6 Dwivedi S P. *Journal of Mechanical Science & Technology*[J], 2014, 28(1): 285
- 7 Xu W F, Liu J H, Zhu H Q et al. *Materials & Design*[J], 2013, 47: 599
- 8 Palanivel R, Koshy Mathews P, Murugan N et al. *Materials & Design*[J], 2012, 40: 7
- 9 Salari E, Jahazi M, Khodabandeh A et al. *Materials & Design* [J], 2014, 58: 381
- 10 Trimble D, O'Donnell G E, Monaghan J. *Journal of Manufacturing Processes*[J], 2015, 17: 141
- 11 Rioja R J, Liu J. *Metallurgical & Materials Transactions A*[J], 2012, 43(9): 3325
- 12 Hamilton C, Dymek S, Blicharski M. *Materials Characterization*[J], 2008, 59(9): 1206
- 13 Mishra R S, Ma Z Y. *Materials Science & Engineering R*[J], 2005, 50(1-2): 1
- 14 Sutton M A, Yang B, Reynolds A P et al. *Materials Science & Engineering A*[J], 2002, 323 (1-2): 160
- 15 Elangovan K, Balasubramanian V. *Materials Science & Engineering A*[J], 2007, 459(1-2): 7
- 16 Avettand-Fenoel M N, Tailliar R. *Metallurgical & Materials Transactions A*[J], 2015, 46(1): 300
- 17 Fonda R W, Bingert J F. *Metallurgical & Materials Transactions A*[J], 2006, 37(12): 3593

## 2195-T8 铝锂合金板材摩擦搅拌焊接头组织与力学性能

李劲风<sup>1</sup>, 陈永来<sup>2</sup>, 张绪虎<sup>2</sup>, 郑子樵<sup>1</sup>

(1. 中南大学, 湖南 长沙 410083)

(2. 航天材料及工艺研究所, 北京 100076)

**摘要:** 采用圆柱状搅拌针及带螺纹圆柱状搅拌针, 进行了5 mm厚度2195-T8铝锂合金板材的摩擦搅拌焊接, 研究了旋转速度及焊接速度对接头拉伸性能的影响, 并检测了接头组织。结果表明, 采用圆柱状搅拌针(旋转速度1000 r/min)进行焊接, 当焊接速度不当时, 产生贯穿焊缝的连续孔洞, 导致接头强度较低。采用带螺纹圆柱状搅拌针进行焊接(焊接速度120 mm/min)时, 可消除上述孔洞缺陷, 且随旋转速度由700 r/min增加至1100 r/min时, 接头强度增大。焊核区晶粒发生再结晶, 但晶粒尺寸分布不均匀。焊核区T1 (Al<sub>2</sub>CuLi)相和 $\theta'$  (Al<sub>2</sub>Cu)相完全溶解, 而热机影响区所有 $\theta'$ 相及大部分T1相溶解。另外, 在焊核心区形成较多位错。

**关键词:** 2195 铝锂合金; 摩擦搅拌焊; 力学性能; 组织

作者简介: 李劲风, 男, 1971年生, 博士, 教授, 中南大学材料科学与工程学院, 湖南 长沙 410083, E-mail: lijinfeng@csu.edu.cn